

ORIGINAL ARTICLE

Magnetic Resonance Imaging

Impact of Filtering on Resolution and Signal-to-Noise Ratio in T2-Weighted

Hamza Arjah MS^{1,2,*}, Noor Diyana Osman¹ PhD*, Hussein ALMasri PhD³, Fawaz Hjouj PhD⁴, Pandji Triadyaksa PhD⁵, Choirul Anam PhD⁵, Mohd Ezane Aziz MD⁶

¹Advanced Medical and Dental Institute, Universiti Sains Malaysia, Kepala Batas, Penang, Malaysia

²Radiology Department, Allmed Medical Center, Ramallah, Palestine

³Medical Imaging Department, Al-Quds University, Abu dis, Jerusalem, Palestine

⁴Mathematics department, Khalifa University, Abu Dhabi, United Arab Emirates

⁵Physics Department, Faculty of Sciences and Mathematics, Universitas Diponegoro,

Jl. Prof. Soedarto SH, Tembalang, Semarang 50275, Central Java, Indonesia

⁶Department of Radiology, School of Medical Sciences, Universiti Sains Malaysia, Kubang Kerian, Kelantan, Malaysia

SUBMISSION: 15/07/2024 - ACCEPTANCE: 08/11/2024

ABSTRACT

Purpose: Image filtering affects image quality in magnetic resonance imaging (MRI). Different filtering techniques are applied in MRI, such as the K-space filter, signal filter, and pixel interpolation. This study aims to evaluate the effects of various filtering approaches on image resolution and signal-to-noise ratio (SNR).

Material and Methods: The modulation transfer function (MTF) for T2 weighted image (T2-w) is employed as a quantitative method to represent spatial resolution and signal-to-noise (SNR) ratio according to the National Electrical Manufacturers Association

(NEMA). In this work, different filtering is applied prospectively. The ImageJ software employed to measures MTF, while the image QC determines SNR.

Results: the normal k-space without filter provides modulation transfer function at 10% (MTF₁₀), the same as the raw and elliptical filters; the MTF₁₀ was around 0.41. However, the MTF at 50% (MTF₅₀) shows more differentiation between K-space filters. signal filters exhibit more difference at, MTF₅₀, the scan without signal filter exhibit highest MTF₅₀ that reach 0.29, while the MTF₅₀ for B1 filter and pre-scan normalization around 0.16. The pixel



Corresponding Author, Guarantor . Hamza Arjah

Email: hamza.arejeh@gmail.com

Phone: 00972597266724

- ¹ Advanced Medical and Dental Institute, Universiti Sains Malaysia, Kepala Batas, Penang, Malaysia
- ² Radiology Department, Allmed Medical Center, Ramallah, Palestine



interpolation mostly doesn't affect MTF₅₀ except for the no signal filter; the MTF₅₀ exhibits pronounced reduction. For SNR, the elliptical filter exhibits lower SNR than the normal k-space, with the highest value equal to 123%. In comparison, the normal k-space without filter provides the highest value, equal to 130%, and the raw filter provides the highest SNR value, equal to 167%. For the signal filter effect on SNR, the B1 filter improves the SNR, while the broad range pre-scan normalisation exhibits less im-

provement for SNR. For pixel interpolation, the SNR is mostly enhanced.

Conclusion: In conclusion, the study underscores the meticulousness required in selecting appropriate MRI filters. The significant influence of filters on image signal and resolution in MRI image processing cannot be excluded. Each filter choice must be carefully tailored to the specific imaging needs, considering the tradeoffs between resolution and SNR.



Signal-to-noise ratio, Modulation transfer function, K-space, MRI filter

Introduction

MRI scanners do not employ ionizing radiation during patient scanning. However, it doesn't mean it possesses no risks, and safety issues exist. Safety culture for the population is inherent in using X-rays and radiation risk [1]. One of the risks of MRI is misdiagnosis. Because misdiagnosis can put a patient's life in danger [2]. MRI scanners should undergo periodic assessments and service checks to eliminate some artifacts that persist unnoticed due to unprofessional manufacturer quality checks and drift from the scanner calibration settings. the quality control (QC) protocols based on phantom assessment can help detect these issues that deteriorate image quality early in the scanning or processing stream [3]. QC includes inspections that ensure readouts match a specific set of standards. In MRI, we can notice multiple numbers of potential artefacts that must be identified to exclude problematic images [4] or corrected as suggested by some QC reports [4]. Among the MRI phantom test items, the high contrast spatial resolution section which is assessed visually, so the test's accuracy can be low [4]. Because the observer previously knows the shape of the objects and differences in observer opinions lead to subjective bias [5], These issues can be eliminated when MTF is calculated. However, there is no adopted value for MTF as a reference in MRI as CT. However, the MRI resolution can be assessed by MTF [6]. The MTF 10 is related to the scanner's ability to detect small objects, while MTF50 is related to visual resolution or apparent sharpness [7]. The SNR is an essential quantitative parameter used to describe the performance of MRI scanners and clinical image quality. SNR is usually used for image assessments and comparison of different radiofrequency (RF) coils and pulse sequences. Various methods have been proposed to determine the MR image SNR [8].

The MRI scanner includes filters for h-space, such as the elliptical filter, which avoids k-space corners compared to no k-space filter; this filter employs a shutter to remove k-space corners [9]. The Raw filter removes the outer line of the raw data matrix and removes the edge oscillation by weighing specific lines. The edge removal is the main parameter that enhances SNR in this filter [10]. Also, the MRI includes signal filters such as the B1 filter, which Is a homogeneous filter used to eliminate signal intensity (SI) differences in MRI images related to dielectric resonance [10] and the Pre-scan normalisation filter which improves SI decay, that is caused by the coil profile [23] However, signal filters are used to correct percentage of image uniformity (PIU) [11]. The MRI include Pixel Interpolation, which Doubles the number of pixels and reduces voxel size without modifying scanning time. Interpolation smooths the resulting image and removes the apparent pixel edge [10].

The image resolution and SNR are affected by different k-space filter [12], and there is a different filtering approach adopted in Siemens MRI scanners, and these filters can be combined with other [13], so the SNR and resolution need to be assessed to provide background knowledge



about the effects of different filtering approaches on SNR and resolution using QC phantom and software.

Material and Methods

Scanner and Phantom

Siemens MRI homogenous Phantom tests were done on a 1.5 tesla (T) MRI system (MAGNETOM ESSENZ with Tim+Dot system; Siemens Medical Solutions, Germany). Acquisitions were performed for three k-space filtering approaches, in combination with signal filters and pixel interpolation algorithm [14]. The used pulse sequence is a T2-w image, a 16-channel Head/Neck coil, and different reconstruction techniques, as described in Table 1. The interpolation can be applied or not. Turning on means the interpolation is applied while turning off means it isn't used.

The pulse sequence used was T2 turbo spin echo (TSE), with all scanning parameters fixed, and the TR used was 8130 milliseconds (ms). Various filters were studied, as summarised in Table 1. At the same time, the used TE is 90 ms, the acquisition matrix 384 * 288, the voxel size is 0.70.75 mm, the turbo factor is 17, the field of view (FOV) is 250 millimetres (mm), and the number of excitations is 1. The homogenous water phantoms include per 1000 gram (g) H2O: 1.24 g NiSO4 x 6H2O + 2.62 g NaCl [15]. Two homogenous water phantoms are placed inside 16-chan-

Table (1): Different reconstruction techniques
in combination with various filtering studied
in this work.

K-space filter	Signal filter	interpolation	
No K-space filter	B1 filter	on	off
	Pre-scan normalization	on	off
	No signal filter	on	off
Elliptical filter	B1 filter	on	off
	Pre-scan normalization	on	off
	No signal filter	on	off
Raw filter	B1 filter	on	off
	Pre-scan normalization	on	off
	No signal filter	on	off

nel Head/Neck coil. The measurements include the circular phantom used for SNR measurements and the rectangular phantom placed on its angle used for resolution assessment of the phantoms shown in Fig. 1. The phantom is placed on its angle to form a slanted edge (SE), and the SE is needed by the algorithm, to measure MTF.



Fig.1: MAGNETOM ESSENZA with Tim + Dot system 1.5 Teslas and two homogenous water phantom inside 16-channel Head/Neck coil. The right image includes the circular phantom that used for SNR measurements, and the left image includes rectangular phantom used for resolution determination.



Signal-to-Noise Ratio (SNR) measurements

SNR measurements were done using two uniform images of a homogeneous phantom obtained with a single acquisition of 28 slices. Then, the images were subtracted, and the software image QC v2.05 performed the subtraction of the images. The software arranges the images and subtracts image 1 from image 2, image 3 from image 4, and so on. The measurements were done by the region of interest (ROI) placed in the phantom center. The SNR was measured according to Equation 1.

$$\frac{SNR = (\sqrt{2*\mu})}{\sigma}$$

Where μ is the mean signal intensity (SI) of the two ROI in two images, and σ is the standard deviation (SD) of the subtracted image [16]. This work used 28 slices, and after the subtraction, the image QC software provided 14 values for subtraction, which were averaged and calculated using Microsoft Excel. To provide the average SNR according to the report (NEMA MS-1 2008) [16].

NEMA recommends calculating μ and σ using a single large ROI, covering at least 75% of the area of the phantom to avoid edge effects [17]. The employed phantom size is 100 mm, while the applied ROI size is 75 mm as shown in Fig. 2.

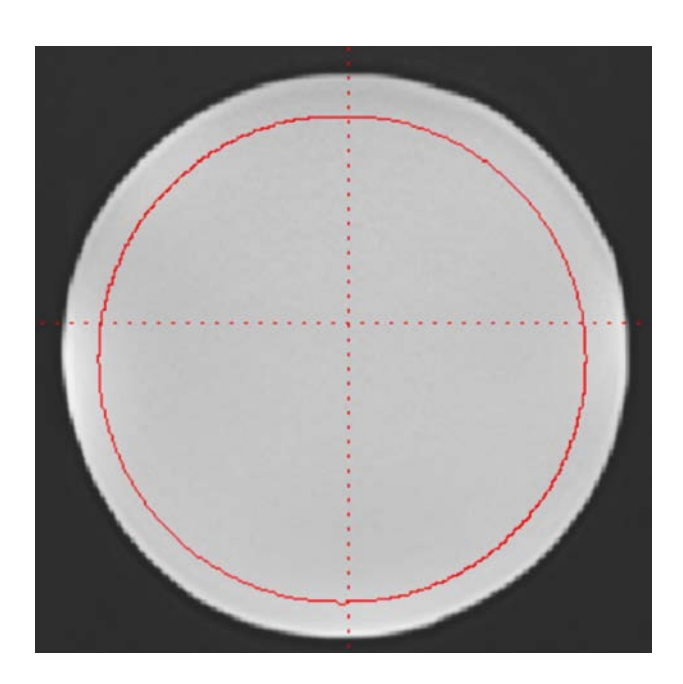


Fig.2: 75 millimetres (mm) region of interest (ROI) placed automatically inside the homogenous phantom image to measure the signal-to-noise ratio (SNR).

Modulation Transfer Function (MTF) measurements

The MTF was measured by ImageJ software, and the SE MTF (SE_MTF) tool was placed in software plugins to measure MTF [18]. The obtained MTF frequency value is distributed in cycles per pixel on the x-axis, while the modulation factor is represented on the y-axis. The values obtained for MTF were saved as an Excel file, and Microsoft Excel was used to draw the MTF curve.

MTF calculations include four plots labelled with short for Sampling Periodicity (SPP), edge spread function (ESF), line spread function (LSF), and MTF curve. The SPP is the result of applying the Fourier transform (FT) Function to the series of the highest values of the LSF applied in the MTF; the MTF is calculated from selected rows of pixels. However, the frequency cycle/pixel is used for digital cameras [19]. And suggested for MRI by some studies. [4], [20], [21]. Because it helps understand the effect of the processing steps that are applied and performed on the obtained image [19]. However, The SE MTF measurements algorithm proposed by the work published by Yongjie Wu et all [22].

MTF measurement tool requires the dark side to be on the left and the bright side to be on the right [22]. As



shown in Fig. 3, the ROI should be rectangular or linear. The applied sample size is 32 pixels to a slanted linear ROI, and the measurement is repeated on five slices. The

28 slices are arranged, and the MTF is measured on slices 5, 10, 15, 20, and 25. The average MTF curve for the five measurements is calculated by Microsoft Excel.

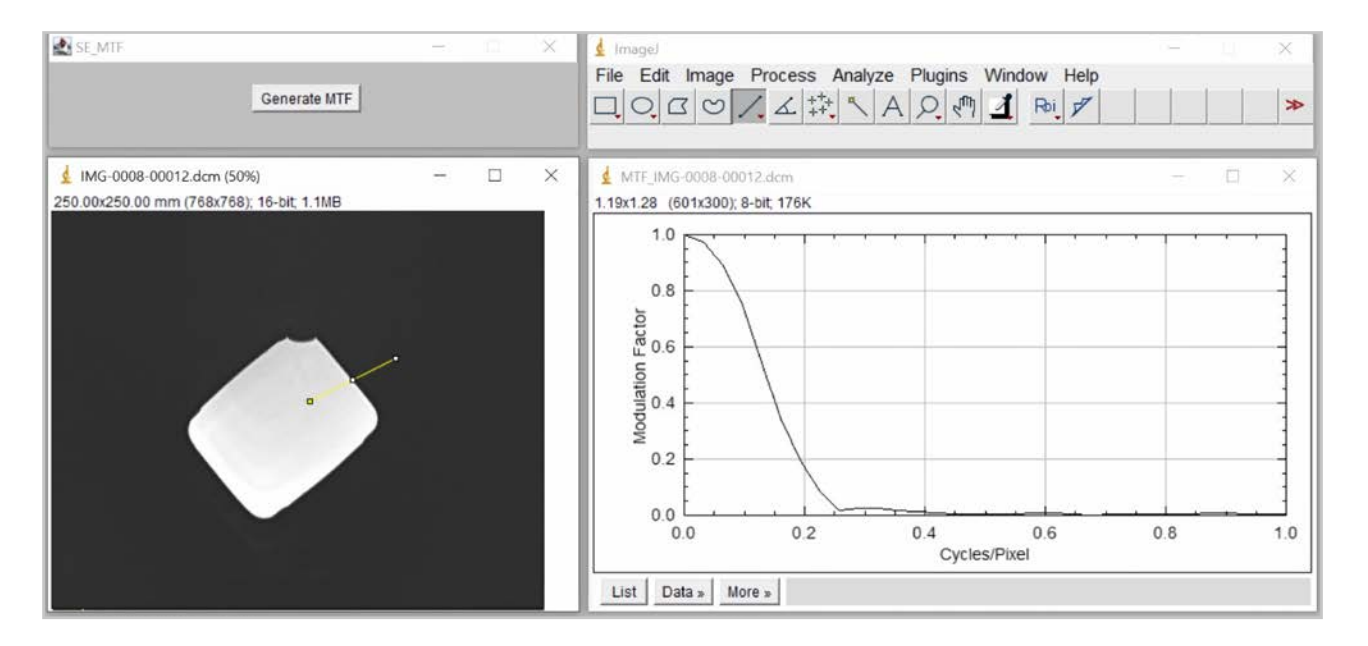


Fig.3: Modulation transfer function (MTF) tool in ImageJ software.

Results

MTF Curves for Standard K-space

The shown MTF curve in Fig. 4 ensures that signal filtering and interpolation affect the MTF curve. In standard k-space without pixel interpolation, the curves overlapped at the area of MTF₁₀ while exhibiting different positions at the area of MTF₅₀; the MTF₁₀ is around 0.41 Cycles/Pixel, for MTF₅₀ the no signal filter MTF₅₀ is 0.29 Cycles/Pixel while B1 filter 0.17 Cycles/Pixel and pre-scan normalisation is 0.16 Cycles/Pixel. After pixel interpolation, the curves overlapped at the area of MTF₅₀ and separated at the area of MTF₁₀; the MTF₅₀ is around 0.16 Cycles/Pixel while MTF₁₀ is worsened for no signal filter and shifted to left from 0.41 Cycles/Pixel to 0.24 Cycles/Pixel.

MTF Curves for Elliptical filter

The plotted MTF curves in Fig. 5 for the elliptical filter show that, for images without pixel interpolation, the curves overlapped at the area of MTF₁₀ while separated at the area of MTF₅₀; the MTF₁₀ is around 0.41 Cycles/Pixel, for MTF₅₀ the no signal filter MTF₅₀ is 0.28 Cycles/Pixel while B1 filter and pre-scan normalisation MTF₅₀ is 0.16 Cycles/Pixel. After pixel interpolation, the curves at the area of MTF₅₀ possess convergent position's and sep-

arated at the area of MTF₁₀; the MTF₅₀ is 0.15 Cycles/Pixel for no signal filter, and 0.16 Cycles/Pixel for B1 filter, and 0.17 Cycles/Pixel for pre-scan normalization; while MTF₁₀ is worsened for no signal filter and shifted to left from to 0.25 Cycles/Pixel compared to B1 filter and prescan normalisation both possess MTF₁₀ of 0.41.

MTF Curves for Raw filter

MTF curves for raw filter were plotted in Fig. 6. For images without pixel interpolation, the curves show overlapping at MTF₁₀ frequency, while separated at MTF₅₀ frequency; the MTF₁₀ is around 0.41 Cycles/Pixel for the three signal filters, while MTF₅₀ exhibited different values; the no signal filter MTF50 is 0.26 Cycles/Pixel while B1 filter is 0.16 and pre-scan normalisation is 0.15 Cycles/Pixel. After pixel interpolation, the curves at the area of MTF₅₀ possess approximately the same position and the curve's positions exhibited more difference at the area of MTF10; the MTF50 is 0.16 Cycles/Pixel for no signal filter, and 0.17 Cycles/Pixel for B1 filter and prescan normalization the MTF₅₀ is 0.16 Cycles/Pixel; The MTF₁₀ for no signal filter and shifted to left from to 0.24 Cycles/Pixel on other hand B1 filter and pre-scan normalisation both possess MTF10 of 0.41 Cycles/Pixel.



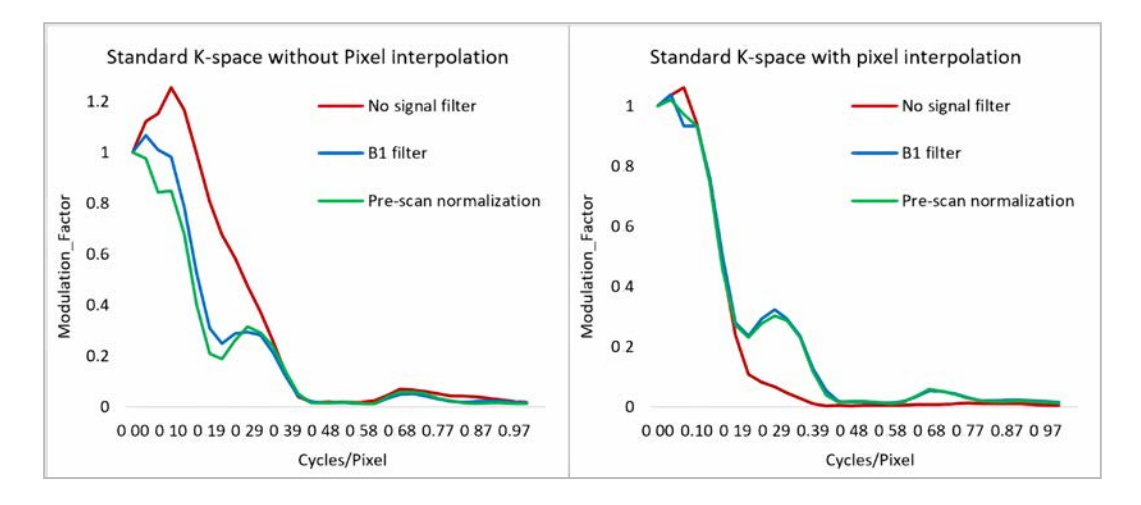


Fig.4: Modulation transfer function (MTF) curves for no K-space filtering with and without interpolation.

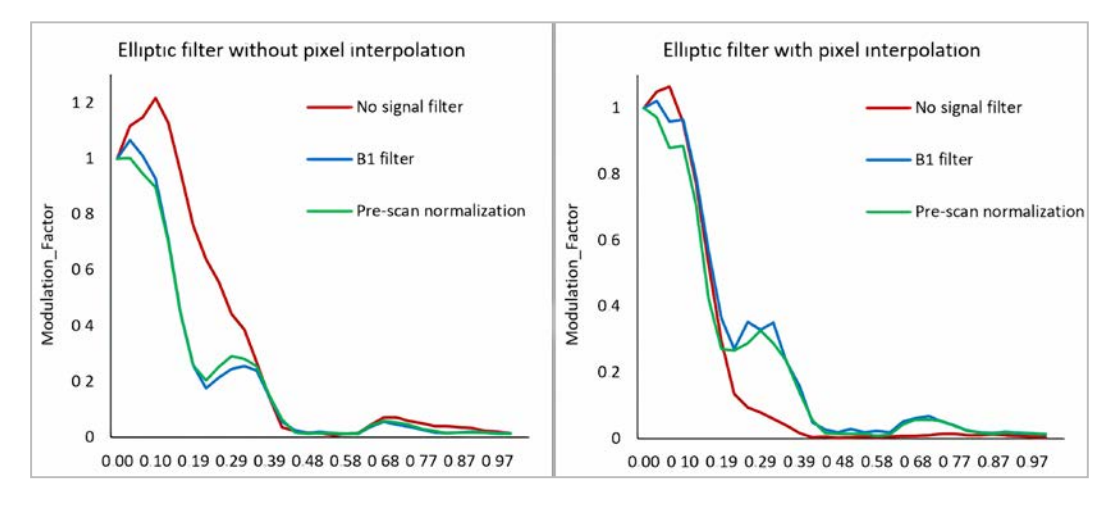


Fig.5: Modulation transfer function curves (MTF) curves for elliptical filter with and without interpolation.

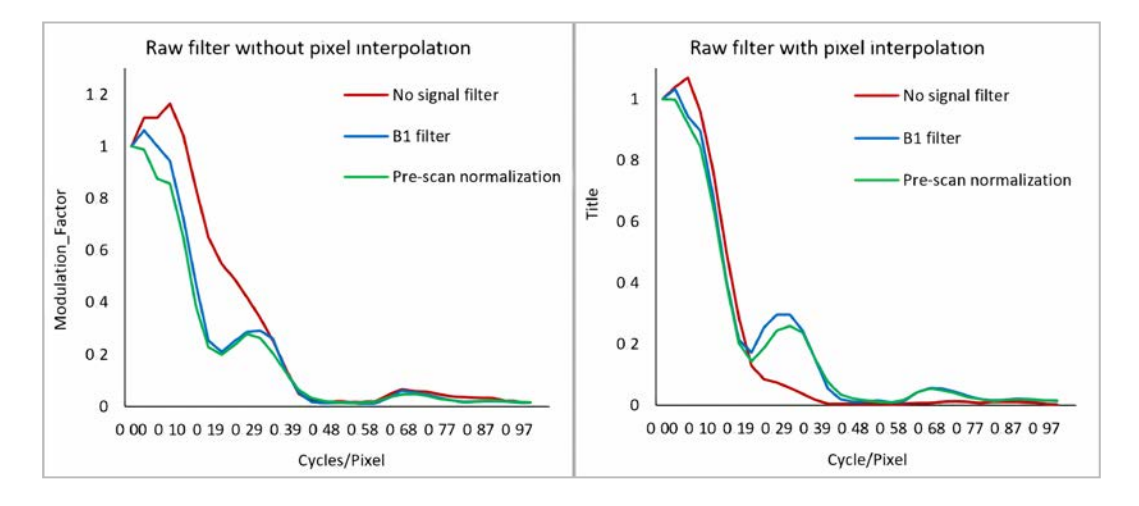


Fig.6: Modulation transfer function (MTF) curves for raw filter with and without interpolation.



SNR for Standard K-space

Fig. 7 shows the SNR for no k-space filter, and the obtained results show that the interpolation enhanced it. The standard image without signal filtering isn't affected significantly by interpolation and possesses a slight increase in SNR. The pre-scan normalisation exhibits more enhancement for SNR compared to the B1 filter.

SNR for images with elliptical filter

Fig. 8 shows the SNR for the elliptical filter, which is slightly reduced compared to an image without a k-space filter. The interpolation algorithm slightly reduced the SNR for an image with no signal filter compared with an image with no interpolation. The pre-scan normalisation exhibits more enhancement for SNR compared to the B1 filter.

SNR for images with raw filter

The highest obtained SNR in this work is for raw filter, as shown in Fig. 9; the SNR is higher than that obtained in standard k-space and elliptical filter. The effects of interpolation are more enhancement for SNR for the three signal filters. Also, the pre-scan normalization exhibits more SNR enhancement than the B1 filter.

The correlation between Carotid Doppler indices and National Institute of Health Sciences stroke scale is represented in (Table 3) shows strong positive correlation (r=0.793, p<0.001), between higher NIHSS Stroke Scale (NIHSS) scores are associated with increased right ICA-EDV. Moderate positive correlation (r=0.439, p<0.001), suggesting a relationship between higher NI-HSS scores and increased left IMT. Strong positive correlation (r=0.926, p<0.001), revealing that elevated NI-HSS scores are associated with increased right ECA-PSV. Weak negative correlation (r=-0.090, p=0.447), indicating a non-significant relationship between left CCA-PSV and NIHSS scores. Strong positive correlation (r=0.654, p<0.001), suggesting that higher NIHSS scores are associated with increased left ICA-PSV. Strong positive correlation (r=0.926, p<0.001), indicating an association between higher NIHSS scores and increased right ECA-PSV. Strong positive correlation (r=0.537, p<0.001), showing a relationship between increased right ICA-EDV and left IMT. Moderate positive correlation (r=0.375, p=0.001), suggesting a relationship between left CCA-PSV and left ICA-PSV. Strong positive correlation (r=0.827, p<0.001), indicating an association between increased right ICA- PSV and right ECA-PSV. Strong positive correlation (r=0.886, p<0.001), showing a relationship between increased left ICA-EDV and right ECA-PSV.

According to (Table 4), the mean IMT significantly varies across groups (p=0.000), indicating differences in the thickness of the right carotid artery wall. Similar to the right side, the left IMT shows significant differences (p=0.001) among the groups, suggesting variations in the thickness of the left carotid artery wall. No significant difference is observed in the right CCA-PSV (p=0.860), implying relatively consistent peak systolic velocity in the common carotid artery. There is a significant difference in the right ICA-EDV (p=0.004), indicating variations in end-diastolic velocity in the right internal carotid artery. No significant difference is found in the left ICA-PSV (p=0.530), suggesting consistent peak systolic velocity in the left internal carotid artery. Similar to the left side, the right ICA-PSV shows no significant difference (p=0.223) among the groups. Significant differences in the left CCA-PSV (p=0.032) indicate variations in peak systolic velocity in the common carotid artery. The mean ECA-PSV is significantly different (p=0.010) among the groups, suggesting variations in peak systolic velocity in the external carotid artery. The ICAA\CCA PSV ratio exhibits significant differences (p=0.159), indicating variations in the ratio of peak systolic velocities between the internal and common carotid arteries. Significant differences in the left ICA-EDV (p=0.030) suggest variations in end-diastolic velocity in the left internal carotid artery. The mean ECA-PSV on the left side is significantly different (p=0.012), indicating variations in peak systolic velocity in the left external carotid artery (Table 4).

Discussion

MTF curves are used with linear array scanners [19]. However, the assessment of MRI spatial resolution by MTF cannot be ensured because the SI has the disadvantage that the linearity of the MRI system cannot be guaranteed [23]. However, the work published by Lim Woo-Taek et al. concludes that MTF can be helpful as a quantitative index and standardised determination method in the QC of MRI spatial resolution [4], in their work, they used the ImageJ software and the Cycles/Pixel frequency distribution to assess MRI resolution using MTF, and they concluded that the MTF measurement could accurately distinguish between low spatial resolution and high spatial resolution [4].



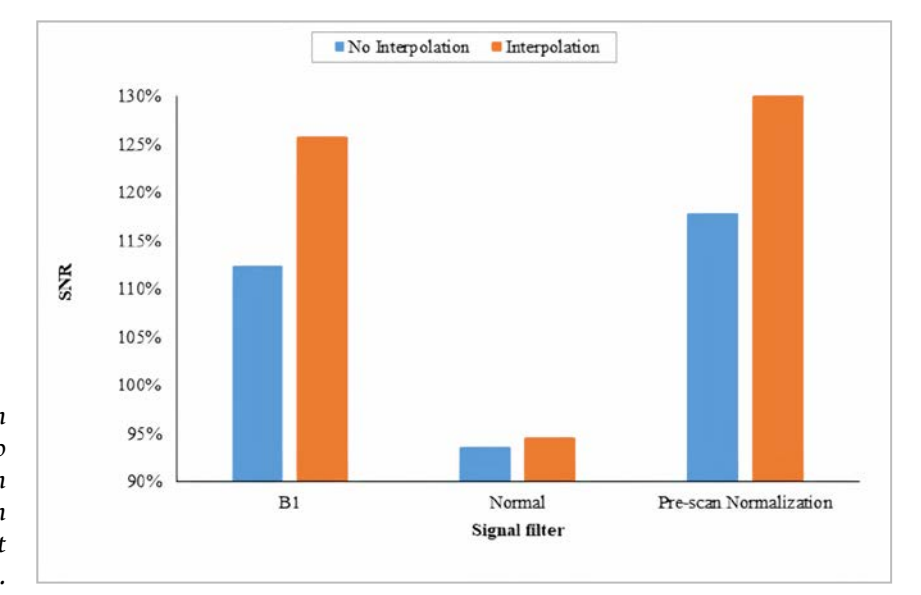


Fig.7: The comparison of signal-to-noise ratio (SNR) values for image with and without interpolation (without k-space filter, but with various signal filter).

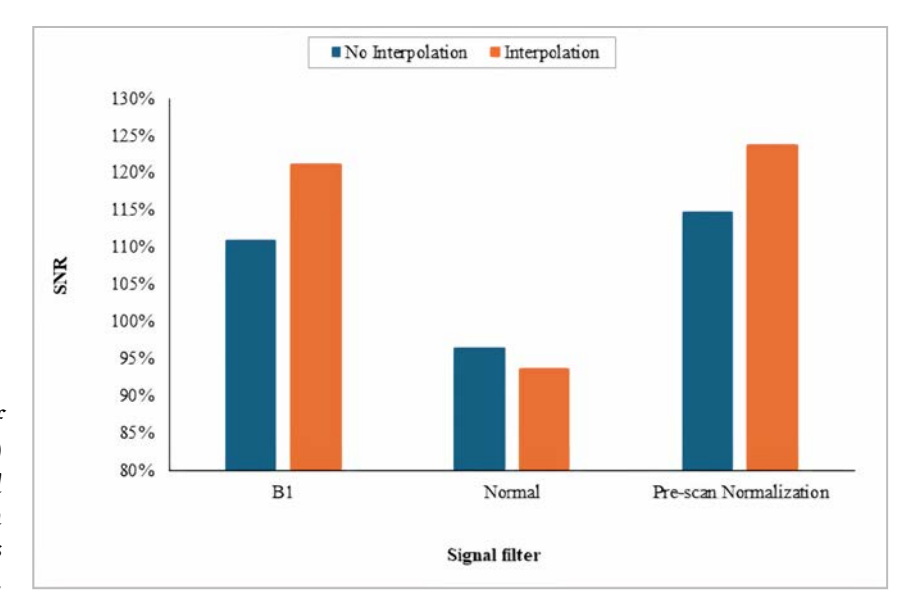


Fig.8: The comparison of signal-to-noise ratio (SNR) values for image with and without interpolation (with elliptical filter and various signal filter).

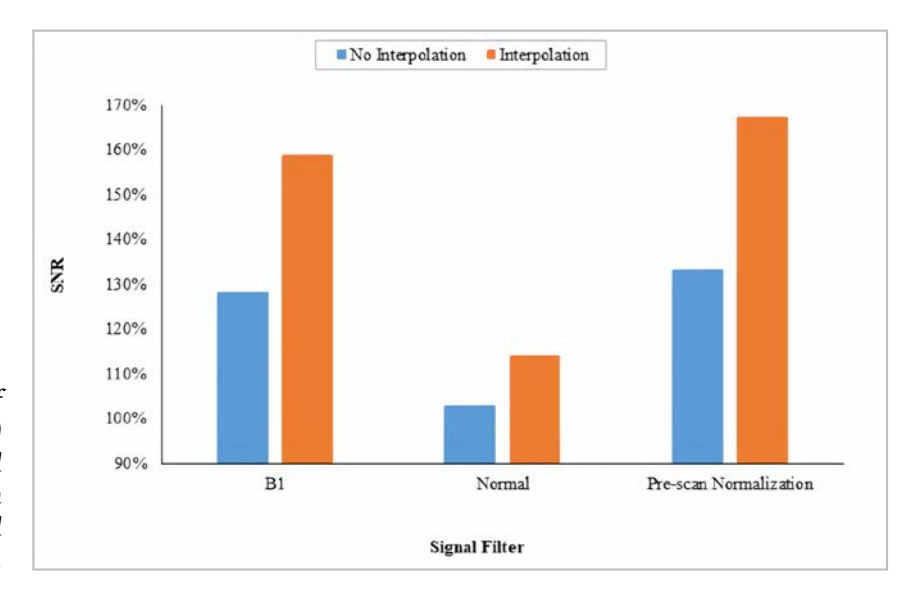


Fig.9: The comparison of signal-to-noise ratio (SNR) values for image with and without interpolation (with raw filter and various signal filter).



The MTF₁₀ is an index for the scanner's ability to detect small objects and its doesn't modified for different k-space filters which mean the scanner ability to detect small objects doesn't modified for different k-Space filters, and the MTF₅₀ is the index for visual apparent resolution of the human and the standard k-space without filtering exhibited the highest apparent resolution with highest MTF₅₀ value of 0.29 Cycles/Pixel, the elliptical filter slightly worsened the apparent resolution compared to standard k-space with highest value of 0.28 Cycles/Pixel, and for raw filter, it is exhibited more worsening for visual resolution with highest MTF₅₀ value of 0.26 Cycles/Pixel.

For signal filters, the most affected is no signal filter curve, while the B1 filter and pre-scan normalisation are not affected significantly by the k-space filter or pixel interpolation. the visual apparent resolution enhanced for no signal filter without pixel interpolation in the three k-space filter, and after interpolation the no signal filter exhibit worsening for scanner ability to detect small objects, the MTF₁₀ is degraded from 0.41 Cycles/Pixel to around 0.25 Cycles/Pixel in the three k-space filters.

The SNR and resolution exhibit an inverse relationship in MRI [24]. For interpolation algorithms, the SNR mostly increased while the MTF worsened. The MTF worsened due to the smoothing process that resulted from pixel edge minimization [14]; however, the SNR was enhanced

due to image smoothing. The SNR for the raw filter was the highest among the three filters, while the apparent resolution was the lowest; the elliptical filter possesses a slight difference in SNR and apparent resolution compared to standard k-space. However, the signal filters increase the SNR compared to the no signal filter, while these filters worsen the apparent resolution. The B1 filter possesses a lower SNR than pre-scan normalisation and a higher visual apparent resolution.

Conclusion:

MRI filtering affects image resolution and SNR. Filtering can enhance SNR without affecting scanning times. The filter should be selected carefully when generating an MRI protocol. The filter can also be used to correct the image SNR and resolution in reconstruction without repeating the sequence.

K-space filters don't exhibit significant differences in the ability of the scanner to detect small objects, while both the raw filter and elliptical filter enhance the SNR and worsen the visual apparent resolution compared to standard k-space without filtering. The B1 and pre-scan normalisation enhance SNR and don't affect the scanner's ability to detect small objects while worsening the visual appearance resolution compared to no signal filter. And finally, The pixel interpolation algorithm mostly worsens the resolution and enhances SNR. R

REFERENCES

- H. Arjah, M. Hjouj, and F. Hjouj, "Low Dose Brain CT, Comparative Study with Brain Post Processing Algorithm," in Proceedings of the 2019 2nd International Conference on Digital Medicine and Image Processing, New York, NY, USA: ACM, Nov. 2019, pp. 1–7. doi: 10.1145/3379299.3379308.
- 2. A. C. Epistatou, I. A. Tsalafoutas, and K. K. Delibasis, "An Automated Method for Quality Control in MRI Systems: Methods and Considerations," J. Imaging, vol. 6, no. 10, p. 111, Oct. 2020, doi: 10.3390/jimaging6100111.
- 3. O. Esteban, D. Birman, M. Schaer, O. O. Koyejo, R. A. Poldrack, and K. J. Gorgolewski, "MRIQC: Advancing the automatic prediction of image quality in MRI from unseen sites," PLoS One, vol. 12, no. 9, p. e0184661, Sep. 2017, doi: 10.1371/journal.pone.0184661.

- W.-T. Lim and H.-R. Jung, "Evaluation on Availability of MTF Measurement Using the ACR Phantom in MRI," Indian J. Sci. Technol., vol. 9, no. S1, pp. 48–52, Dec. 2016, doi: 10.17485/ijst/2016/v9iS1/109836.
- A. Omigbodun, J. Y. Vaishnav, and S. S. Hsieh, "Rapid measurement of the low contrast detectability of CT scanners," Med. Phys., vol. 48, no. 3, pp. 1054–1063, Mar. 2021, doi: 10.1002/mp.14657.
- 6. R. R. Price et al., "Quality assurance methods and phantoms for magnetic resonance imaging: Report of AAPM nuclear magnetic resonance Task Group No. 1," Med. Phys., vol. 17, no. 2, pp. 287–295, Mar. 1990, doi: 10.1118/1.596566.
- H.-W. Cho, H.-J. Yoon, and J.-C. Yoon, "Analysis of Crack Image Recognition Characteristics in Concrete Structures Depending on the Illumination and Im-



- age Acquisition Distance through Outdoor Experiments," Sensors, vol. 16, no. 10, p. 1646, Oct. 2016, doi: 10.3390/s16101646.
- 8. O. Dietrich, J. G. Raya, S. B. Reeder, M. F. Reiser, and S. O. Schoenberg, "Measurement of signal-to-noise ratios in MR images: Influence of multichannel coils, parallel imaging, and reconstruction filters," J. Magn. Reson. Imaging, vol. 26, no. 2, pp. 375–385, Aug. 2007, doi: 10.1002/jmri.20969.
- 9. C. Pereira, "MRI (1.5 and 3 Tesla) Sequence Optimization for Use in Orthopaedics," p. 174, 2016.
- 10. H. Sector, "syngo MR D14," 2010.
- 11. R. Price et al., "Magnetic Resonance Imaging Quality Control Manual 2015," 2015. [Online]. Available: https://www.acr.org/-/media/ACR/Files/Clinical-Resources/QC-Manuals/MR_QCManual.pdf
- 12. [C. Ciulla, "Intensity-curvature functional-based filtering in image space and k-space: Applications in magnetic resonance imaging of the human brain," High Freq., vol. 2, no. 1, pp. 48–60, Feb. 2019, doi: 10.1002/hf2.10031.
- 13. J. W. Meisingset, "Magnetic Resonance Imaging: Multidimensional non-Gaussian Diffusion-weighted MRI Image quality analysis Jens Wergeland Meisingset," Norwegian University of Science and Technology, 2015. [Online]. Available: https://ntnuopen.ntnu.no/ntnu-xmlui/handle/11250/2352158
- 14. M. A. Bernstein, S. B. Fain, and S. J. Riederer, "Effect of windowing and zero-filled reconstruction of MRI data on spatial resolution and acquisition strategy," J. Magn. Reson. Imaging, vol. 14, no. 3, pp. 270–280, Sep. 2001, doi: 10.1002/jmri.1183.
- C. Liu et al., "Diurnal Variation in Hydration of the Cervical Intervertebral Disc Assessed Using T2 Mapping of Magnetic Resonance Imaging," Korean J. Radiol., vol. 23, no. 6, pp. 638–648, 2022, doi: 10.3348/kjr.2021.0950.
- 16. NEMA, "NEMA Standards Publication MS 3-2008: Determination of Image Uniformity in Diagnostic Magnetic Resonance Imaging," 2021. [Online]. Available:

- https://www.nema.org/standards/view/determination-of-image-uniformity-in-diagnostic-magnetic-resonance-images
- 17. J. Harkin and C. Ingham, "Comparison of SNR Assessment Techniques for Routine Multi-Element RF Coil QC Testing," IPEM-Translation, vol. 2, p. 100012, Jul. 2022, doi: 10.1016/j.ipemt.2022.100012.
- C. A. Corum, S. J. Kruger, and V. A. Magnotta, "HEAL-Pix View-order for 3D Radial Self-Navigated Motion-Corrected ZTE MRI," arXiv Med. Phys., pp. 8–11, Oct. 2019, [Online]. Available: https://api.semanticscholar.org/CorpusID:204838337
- 19. D. Williams and P. D. Burns, "Diagnostics for Digital Capture using MTF," Soc. Imaging Sci. Technol. Image Process. Image Qual. Image Capture, Syst. Conf., pp. 227–232, 2001.
- 20. M. Kikuchi et al., "MTF Measurement of MR Blurring in Liver Dynamic MRI with Gd-EOB-DTPA," Japanese J. Radiol. Technol., vol. 72, no. 11, pp. 1169–1176, 2016, doi: 10.6009/jjrt.2016_JSRT_72.11.1169.
- 21. T. Y, U. T, M. T, and Y. K, "Comparison between Linear and Reverse Linear K-Space Order with Partial Fourier Fractions for Modulation Transfer Function in Dynamic Contrast-Enhanced Magnetic Resonance Imaging: A Simulation Study," J. Comput. Sci. Syst. Biol., vol. 10, no. 3, pp. 28–31, 2017, doi: 10.4172/jcsb.1000245.
- 22. Y. Wu, W. Xu, Y. Piao, and W. Yue, "Analysis of Edge Method Accuracy and Practical Multidirectional Modulation Transfer Function Measurement," Appl. Sci., vol. 12, no. 24, p. 12748, Dec. 2022, doi: 10.3390/app122412748.
- 23. N. Koori et al., "Influence of half Fourier and elliptical scanning (radial scan) on magnetic resonance images," J. Magn. Reson., vol. 355, p. 107560, Oct. 2023, doi: 10.1016/j.jmr.2023.107560.
- 24. W. Zafar, "Resolution, SNR, Signal Averaging and Scan Time in MRI for Metastatic Lesion in Spine: A Case Report in a 74 Years Old Patient," Clin. Radiol. Imaging J., vol. 3, no. 1, 2019, doi: 10.23880/CRIJ-16000139.



Hamza Arjah MS, Noor Diyana Osman PhD, Fawaz Hjouj PhD, Hussein ALMasri PhD, Pandji Triadyaksa PhD, Choirul Anam PhD, Mohd Ezane Aziz MD. Impact of Filtering on Resolution and Signal-to-Noise Ratio in T2-Weighted, *Hell J Radiol* 2025; 10(2): 24-33.